The viscoelastic reflection/transmission problem for general orientation of propagation and attenuation vectors

J. Brokešová, V. Červený

Department of Geophysics, Charles University, Ke Karlovu 3,
121 16 Praha 2, Czech Republic.
E-mails: johana@seis.karlov.mff.cuni.cz, vcerveny@seis.karlov.mff.cuni.cz

Summary

We consider the reflection/transmission (R/T) problem of inhomogeneous plane waves at a plane interface between two homogeneous isotropic viscoelastic halfspaces. A general orientation of the attenuation vector of the incident wave is allowed, even orientation away from the plane of incidence. A procedure of determining the complex-valued normal components of the slowness vectors of generated reflected/transmitted waves from the tangential components of these vectors, known along the interface, is proposed. Particular attention is devoted to the determination of the sign of complex-valued square roots, involved in the problem. Continuity criteria are proposed, which are based on the requirement that the vertical components of the slowness vectors of generated waves must be continuous along a parametric line in the complex-valued plane of tangential components of the slowness vector, along which we wish to calculate the R/T coefficients. For example, if we wish to compute the R/T coefficients versus the incidence propagation angle, we choose the parameter along the parametric line to represent the incidence propagation angle. The criteria remove the non-physical jumps of the vertical components of the slowness vectors of generated waves (and, consequently, even the nonphysical jumps in the R/T coefficients), caused by erroneous transition from one sheet of the Riemannian surface to the other.

For the general orientation of the attenuation vector of the incident wave, the system of six boundary conditions at the interface cannot be decomposed into two subsystems, corresponding to P-SV and SH waves. Consequently, all these waves are mutually coupled at structural interfaces due to viscoelasticity. In general, the R/T coefficients are not symmetrical with respect to positive and negative incidence propagation angles. Depending on the behaviour of the tangential components of the attenuation vector, the amplitudes of generated R/T waves may decay exponentially away from the interface for certain incidence propagation angles, and grow exponentially away from the interface for other incidence angles. Similarly, the propagation vectors of generated waves may be oriented towards the interface for certain incidence propagation angles. Consequently, the R/T propagation angles may exceed 90^o.

Key words: viscoelastic media, inhomogeneous waves, reflection, transmission, propagation vector, attenuation vector.

Seismic Waves in Complex 3-D Structures, Report No.12, Department of Geophysics, Charles University, Praha 2002

1 Introduction

In the R/T problem of plane waves at a plane interface between two viscoelastic homogeneous isotropic halfspaces, the basic role is played by the determination of the normal components of the slowness vectors of generated reflected and transmitted plane waves from known tangential components of the slowness vectors. The tangential components of the slowness vectors of all the reflected and transmitted plane waves generated along the interface are presumably known; they equal the tangential components of the slowness vector of the incident wave (Snell's law). A similar problem also appears in many other wave propagation problems, for example, in the determination of the normal components of the slowness vectors of generated waves at an initial plane, along which the tangential components of the initial-value slowness vectors are known.

The solution of the above problems is well known for the elastic case. The viscoelastic description, however, has been found very useful to study wave propagation in certain regions of the Earth's interior, which were of great interest in recent seismology and seismic exploration (for example, shallow consolidated sediments, reservoir rocks, zones of partial melting, mining areas). See Auld (1990), Caviglia and Morro (1992), Carcione (2001), and many other references given in these books. Moreover, even the wave propagation problems in certain more complex types of rocks can be studied using empirical relations, expressing the properties of such rocks in terms of viscoelastic relations, see Koesoemadinata and McMechan (2001a, b). This applies, for example, to porosity, water saturation, and so on.

For these reasons, it would be valuable to generalize the wave propagation techniques, known for elastic media (for example, the seismic ray method), also to viscoelastic media, and to try to understand well the differences between the behaviour of seismic wave fields in elastic and viscoelastic media. This paper presents a contribution to such an effort.

In viscoelastic media, the velocities of propagation and the slowness vectors of plane waves are complex-valued. We can express the slowness vector $\mathbf{p}$ in the following form:

$$\mathbf{p} = \mathbf{P} + \mathrm{i}\mathbf{A}. \tag{1}$$

The real-valued vector $\mathbf{P}$ is usually called the propagation vector, and the real-valued vector $\mathbf{A}$ the attenuation vector. Planes $P_i x_i = const.$ are commonly referred to as planes of constant phases, and planes $A_i x_i = const.$ as planes of constant amplitudes. It is also usual to introduce the attenuation angle γ as the angle between vectors $\mathbf{P}$ and $\mathbf{A}$,

$$\cos\gamma = \mathbf{P}\cdot\mathbf{A}/|\mathbf{P}||\mathbf{A}|. \tag{2}$$

For $\gamma = 0$, the plane wave is called homogeneous, and for $\gamma \neq 0$ inhomogeneous. Consequently, for homogeneous plane waves, $\mathbf{P}$ and $\mathbf{A}$ are parallel. For inhomogeneous plane waves in viscoelastic isotropic media, the attenuation angle is always within the limits $-\frac{1}{2}\pi < \gamma < \frac{1}{2}\pi$. Inhomogeneous plane waves may also exist in elastic isotropic media; then $\gamma = \frac{1}{2}\pi$.

We shall now consider an arbitrarily situated plane Σ, with unit normal $\mathbf{n}$, and decompose slowness vector $\mathbf{p}$ into complex-valued vectorial normal and tangential components,

$$\mathbf{p} = \mathbf{p}^{norm} + \mathbf{p}^{tang}. \tag{3}$$

Analogously to (1), we can separate the real and imaginary parts of both these complex-valued vectors,

$$\mathbf{p}^{norm} = \mathbf{P}^{norm} + \mathrm{i}\mathbf{A}^{norm}, \quad \mathbf{p}^{tang} = \mathbf{P}^{tang} + \mathrm{i}\mathbf{A}^{tang}. \tag{4}$$

Here, $\mathbf{P}^{norm}$, $\mathbf{A}^{norm}$, $\mathbf{P}^{tang}$, and $\mathbf{A}^{tang}$ are real-valued vectors. Similarly as in (2), we can introduce angle δ between $\mathbf{P}^{tang}$ and $\mathbf{A}^{tang}$,

$$\cos\delta = \mathbf{P}^{tang} \cdot \mathbf{A}^{tang} / |\mathbf{P}^{tang}||\mathbf{A}^{tang}|. \tag{5}$$

We shall call δ the tangential attenuation angle. Contrary to γ, the tangential attenuation angle may exceed $\frac{1}{2}\pi$, $-\pi < \delta \leq \pi$. For $\delta = 0$, $\mathbf{P}^{tang}$ and $\mathbf{A}^{tang}$ are parallel. It should be useful to specify the difference between the attenuation angle γ and the tangential attenuation angle δ. For homogeneous plane waves ($\gamma = 0$), the tangential attenuation angle equals 0 or π. On the contrary, $\delta = 0$ does not imply that the plane wave is homogeneous ($\gamma = 0$), but γ may be arbitrary within the limits $-\frac{1}{2}\pi < \gamma < \frac{1}{2}\pi$.

We shall introduce the following terminology. We shall call the situation with coplanar $\mathbf{P}$, $\mathbf{A}$ and $\mathbf{n}$ the *coplanar case*. In the coplanar case, $\mathbf{P}^{tang}$ and $\mathbf{A}^{tang}$ are parallel, so that $\cos\delta = 1$, and $\delta = 0$ or $\delta = \pi$. Analogously, we shall call the general situation with noncoplanar $\mathbf{P}$, $\mathbf{A}$ and $\mathbf{n}$ the *noncoplanar case*. The noncoplanar case corresponds to $\cos\delta \neq 1$. The coplanar case ($\cos\delta = 1$) does not imply that the wave under consideration is homogeneous ($\gamma = 0$), but the homogeneous wave ($\gamma = 0$) implies the parallelity of $\mathbf{P}$, and $\mathbf{A}$ (i.e. $\cos\delta = 1$).

In the R/T problem for viscoelastic media, practically only the coplanar case ($\cos\delta = 1$) has been discussed in the seismological literature. See Borcherdt (1977, 1982), Krebes (1983, 1984), Deschamps (1990, 1993), Ainslie and Burns (1995), Brokešová and Červený (1998), Brokešová (2001), and many other references given in these papers. The assumption of coplanarity of $\mathbf{P}$, $\mathbf{A}$ and $\mathbf{n}$ simplifies the R/T process considerably. The system of equations for R/T coefficients, consisting of six equations, can be decomposed into two subsystems in the coplanar case, one consisting of four and the other one of two equations. The system consisting of four equations is usually called the P-SV (or P- and Type-I S) system, and the system consisting of two equations the SH (or Type-II S) system. To obtain the complete set of R/T coefficients, the P-SV system must be solved twice (for the incident P and incident SV wave), and the SH system must be solved once. Consequently, the complete set of R/T coefficients consists of five reflection and five transmission coefficients. For the noncoplanar case ($\cos\delta \neq 1$), this decomposition is impossible, and the system of six equations must be solved as a whole, similarly as in anisotropic media. To obtain the complete set of R/T coefficients, the system of six equations must be solved three times. Consequently, nine reflection and nine transmission coefficients are obtained. In other words, the P-SV waves are coupled with the SH waves in the R/T process at an interface between two viscoelastic media, if a noncoplanar case is being considered.

In this paper, we shall consistently consider the fully general noncoplanar case of $\cos\delta \neq 1$. The noncoplanar case of $\delta \neq 0$ plays an important role in some practical applications, particularly in 3-D wave propagation problems of viscoelastic layered structures. Main results of this paper are also briefly discussed in Brokešová and Červený (2002).

It is well known (see also Section 2) that the slowness vector of a plane wave propagating in a viscoelastic isotropic medium must satisfy the existence condition, following from the elastodynamic equation:

$$p_1^2 + p_2^2 + p_3^2 = 1/V_C^2. \tag{6}$$

Here p_i are Cartesian components of the slowness vector $\mathbf{p}$ of the plane wave under consideration, and V_C is the complex-valued velocity. Without any loss of generality, we introduce the Cartesian coordinate system x_i in such a way that its origin is situated on plane Σ, and the x_3-axis is normal to Σ, pointing into the halfspace specified by velocity V_C. If Σ represents a structural interface, the velocity on the other side of Σ is different from V_C. In our Cartesian coordinate system, the vectorial tangential component of slowness vector $\mathbf{p}^{tang}$ has Cartesian components p_1, p_2 (with $p_3 = 0$), and the vectorial normal component of slowness vector $\mathbf{p}^{norm}$ has only one non-vanishing component p_3 (with $p_1 = 0, p_2 = 0$). Thus, the determination of the normal component of the slowness vector from its tangential components reduces to the determination of p_3 from known p_1 and p_2. Using (6), we obtain

$$p_3 = \pm\mathcal{P.V.}[1/V_C^2 - p_1^2 - p_2^2]^{1/2}. \tag{7}$$

Here, $\mathcal{P.V.}$ is the principal value. Note that $\mathcal{P.V.}[z]^{1/2}$ is uniquely defined for any complex-valued z. Square root $\sqrt{z}$ is defined on a two-sheeted Riemannian surface, with a branch line constructed from 0 to $-\infty$, along the negative part of the real axis. Then, $\mathcal{P.V.}[z]^{1/2}$ is defined on the upper sheet of the Riemannian surface and corresponds to $\mathrm{Re}[z]^{1/2} \geq 0$. Consequently, the main problem in Eq. (7) consists in the selection of the correct sign.

It is very simple to select the sign in (7) for $\mathbf{A}^{tang} = 0$ and for V_C real-valued. This corresponds, for example, to a homogeneous plane wave incident at interface Σ between two elastic (non-dissipative) isotropic halfspaces. The generated waves are then homogeneous or inhomogeneous. The sign in (7), corresponding to a homogeneous generated wave (with real-valued p_3) is then "+", as the slowness vector of the generated wave is always oriented away from interface Σ. The sign in (7), corresponding to the inhomogeneous generated wave (with imaginary-valued p_3) is then chosen so that the amplitudes decay exponentially away from the interface. Thus, the specification of downgoing and upgoing waves in the R/T process is simple in elastic isotropic media. For viscoelastic isotropic media, however, the sign selection is not so simple. The generated inhomogeneous plane waves in the R/T process may also grow exponentially away from the interface. Moreover, the sign of P_3 is not necessarily positive, but may also be negative. These facts are known well from the coplanar case studies described in the seismological literature, see Buchen (1971), Richards (1981), Krebes (1984), Brokešová and Červený (1998, 2001), Brokešová (2001), and many other references given in these papers.

Note that the determination of p_3 from p_1 and p_2 is simple even in anisotropic elastic media, although it is algebraically more involved than in isotropic elastic media. For

$\mathbf{A}^{tang} = 0$ and real-valued elastic moduli, the possible values of p_3 are obtained from p_1 and p_2 by solving an algebraic equation of the sixth order, which follows from the existence condition for anisotropic media. This equation yields six roots, from which three appropriate roots must be selected (see, Červený, 2001, p. 50 – 51). For homogeneous plane waves generated at Σ, the selection of real-valued roots p_3 is based on the direction of the average energy flux (not on the direction of the slowness vector). It is not surprising that the selection of the sign in (7), based on the direction of the average energy flux, was also tried in viscoelastic isotropic media, see Borcherdt (1973), among others. It was, however, shown that the selection based on the average energy flux also fails in viscoelastic media. See Krebes (1984), and the detailed discussion in Brokešová and Červený (2001).

In this paper, we propose the **continuity criterion** for the selection of the sign in (7) in the viscoelastic media. The continuity criterion is suitable if we wish to compute p_3 along some curve (here called the profile) in the complex-valued $p_1 - p_2$ domain. The most common example of such profile corresponds, e.g., to the computations of R/T coefficients versus the propagation angle of incidence, which varies from 0^o to 90^o. The continuity criterion consists in the requirement that p_3 $(= P_3 + \mathrm{i}A_3)$ is continuous along the whole profile. Consequently, it is required that also the R/T coefficients are continuous along the profile. In the formulation of the criterion, see Section 3, we shall exploit the fact that p_3 changes sign only if the profile crosses the branch line of the square root $[1/V_C^2 - p_1^2 - p_2^2]^{1/2}$. The final criteria are very simple.

A similar criterion for the special case of $p_2 = 0$ was proposed earlier by Krebes (1984), see also Brokešová and Červený (1998) and Brokešová (2001). Actually, the case of $p_2 = 0$ corresponds to the coplanar case ($\cos\delta = 1$). The criterion was successfully applied to extensive computations and discussions of decoupled P-SV and SH coefficients in viscoelastic media in the coplanar case by Brokešová and Červený (1998). Here we shall present the criterion for a general noncoplanar case ($\cos\delta \neq 1$), which can also be used to compute the whole system of eighteen R/T coefficients, including the coupled R/T coefficients P-SV$\rightarrow$SH and SH$\rightarrow$P-SV. The criterion for the coplanar case is, of course, included as a special case.

In the whole paper, the lower-case indices $(i, j, k, \ldots)$ take the values of 1, 2, 3, and the upper-case indices $(I, J, K, \ldots)$ the values of 1, 2. The Einstein summation convention is applied to the repeated indices. We shall consistently distinguish between viscoelastic media (complex-valued velocities) and elastic media (real-valued velocities). A different terminology has also been commonly used in the seismological literature for viscoelastic media to emphasize certain aspects of these media, for example dissipative, anelastic, lossy media, media with attenuation, etc. Similarly, for elastic media, also terms like nondissipative, perfectly elastic, loss-less, without attenuation, etc., have often been used.

2 Determination of the normal component of the slowness vector from its tangential components

We shall consider a homogeneous viscoelastic isotropic medium described, for a fixed positive frequency ω, by complex-valued Lamé's elastic parameters $\lambda = \lambda^R + \mathrm{i}\lambda^I$ and $\mu = \mu^R + \mathrm{i}\mu^I$. The complex-valued velocities of P and S waves, α and β, are given by the relations

$$\alpha^2 = V_P^2(1 - \mathrm{i}/Q_P), \quad \beta^2 = V_S^2(1 - \mathrm{i}/Q_S). \tag{8}$$

Here V_P and V_S are real-valued velocities of P and S waves in relevant elastic medium,

$$V_P = \left(\frac{\lambda^R + 2\mu^R}{\rho}\right)^{1/2}, \quad V_S = \left(\frac{\mu^R}{\rho}\right)^{1/2}, \tag{9}$$

and Q_P and Q_S are quality factors of P and S waves,

$$Q_P = -\frac{\lambda^R + 2\mu^R}{\lambda^I + 2\mu^I}, \quad Q_S = -\frac{\mu^R}{\mu^I}. \tag{10}$$

As the treatment in this paper is quite the same for both P and S waves, we shall use the same notation for both cases. For the wave under consideration, we denote the complex-valued velocity by V_C, the real-valued velocity by V, and the quality factor by Q. The complex-valued velocity V_C is then expressed in terms of V and Q as follows:

$$V_C^2 = V^2(1 - \mathrm{i}/Q). \tag{11}$$

Any time-harmonic plane wave propagating in the viscoelastic isotropic homogeneous medium under consideration can be expressed in the following form:

$$u_i(x_j, t) = U_i \exp[-\mathrm{i}\omega(t - p_k x_k)]. \tag{12}$$

Here $u_i(x_j, t)$ are Cartesian components of the complex-valued displacement vector $\mathbf{u}(x_i, t)$, U_i the Cartesian component of the complex-valued constant amplitude vector $\mathbf{U}$, and p_i the Cartesian components of the complex-valued slowness vector $\mathbf{p}$. The complex-valued slowness vector $\mathbf{p}$ can be expressed in terms of the real-valued propagation vector $\mathbf{P}$ and real-valued attenuation vector $\mathbf{A}$ as shown in (1). Plane wave (12) represents a non-trivial solution of the viscoelastodynamic equation if, and only if, existence condition (6) is satisfied.

At this point, it would be useful to emphasize two important sign conventions used in this paper.

1. The first sign convention applies to the time harmonic plane wave (12), where we have used "$-$" in the exponential term, $\exp[-\mathrm{i}\omega\theta]$ with $\theta = t - p_k x_k$. This sign convention corresponds to the most common sign option used in the seismic ray method, see Červený (2001).

2. The second sign convention corresponds to the assumed orientation of the x_3-axis. This convention, of course, directly influences the sign of p_3. In this paper, we assume that the x_3-axis has the direction of the normal $\mathbf{n}$ to Σ, with $\mathbf{n}$ oriented away from Σ into the halfspace in which the generated plane wave under consideration propagates (described by velocity V_C). Thus, if transmitted waves are discussed, the x_3-axis is oriented into the medium in which the transmitted wave propagates. Analogously, if reflected waves are considered, the x_3-axis is oriented into the medium in which the reflected wave propagates. Only if we wish to consider one coordinate system common to all waves, do we have to modify the signs of p_3 appropriately.

If we separate the real and imaginary parts in (6), we obtain two coupled equations for P_i and A_i,

$$P_iP_i - A_iA_i = V^{-2}(1+Q^{-2})^{-1}, \quad 2P_iA_i = V^{-2}Q^{-1}(1+Q^{-2})^{-1}. \tag{13}$$

Inserting (2) into the second equation of (13), we can solve (13) for $|\mathbf{P}|$ and $|\mathbf{A}|$

$$|\mathbf{P}| = \sqrt{g+1}/\sqrt{2}V\sqrt{1+Q^{-2}}, \quad |\mathbf{A}| = \sqrt{g-1}/\sqrt{2}V\sqrt{1+Q^{-2}}, \tag{14}$$

where

$$g = [1 + Q^{-2}\cos^{-2}\gamma]^{1/2}. \tag{15}$$

Here γ is the attenuation angle given by (2). We can also introduce the real-valued phase velocity of plane wave (12) by the relation

$$\mathcal{C} = 1/|\mathbf{P}| = \sqrt{2}V\sqrt{1+Q^{-2}}/\sqrt{g+1}. \tag{16}$$

It represents the velocity of propagation of the phase front in the direction perpendicular to it.

Now we shall use (13) to determine P_3 and A_3 from known P_1, A_1, P_2 and A_2. We express (13) in the form:

$$\begin{aligned} P_3P_3 - A_3A_3 &= V^{-2}(1+Q^{-2})^{-1} - P_KP_K + A_KA_K, \\ 2P_3A_3 &= V^{-2}Q^{-1}(1+Q^{-2})^{-1} - 2P_KA_K. \end{aligned} \tag{17}$$

Here, the Einstein summation convention is applied to $K = 1, 2$.

It may be convenient to express quantities P_1, A_1, P_2, A_2 in terms of other quantities P, A, δ and ϕ as follows:

$$\begin{aligned} P_1 &= P\cos\phi, & P_2 &= P\sin\phi, \\ A_1 &= A\cos(\phi+\delta), & A_2 &= A\sin(\phi+\delta). \end{aligned} \tag{18}$$

The physical meaning of quantities P, A, ϕ and δ is obvious. P and A are the lengths of vectors $\mathbf{P}^{tang}$ and $\mathbf{A}^{tang}$, $P = |\mathbf{P}^{tang}|$ and $A = |\mathbf{A}^{tang}|$, ϕ is the angle between $\mathbf{P}^{tang}$ and the positive direction of the Cartesian axis x_1, $-\pi < \phi \leq \pi$, and δ is the tangential attenuation angle, $-\pi < \delta \leq \pi$. Using (18), we can determine P_1, A_1, P_2, A_2 from P, A, ϕ and δ, and vice versa. Equation (18) yields

$$P = \sqrt{P_1^2 + P_2^2}, \quad A = \sqrt{A_1^2 + A_2^2}, \tag{19}$$

$$\begin{aligned} \cos\phi &= P_1/P, & \cos\delta &= (P_1A_1 + P_2A_2)/PA, \\ \sin\phi &= P_2/P, & \sin\delta &= (P_1A_2 - P_2A_1)/PA. \end{aligned} \tag{20}$$

Consequently, the system of two equations (17) for P_3 and A_3 can be expressed in the following simple form:

$$P_3^2 - A_3^2 = a, \quad 2P_3A_3 = b, \tag{21}$$

where

$$
\begin{aligned}
a &= V^{-2}(1+Q^{-2})^{-1} - P_1^2 - P_2^2 + A_1^2 + A_2^2 = V^{-2}(1+Q^{-2})^{-1} - P^2 + A^2, \\
b &= V^{-2}Q^{-1}(1+Q^{-2})^{-1} - 2(P_1A_1 + P_2A_2) = V^{-2}Q^{-1}(1+Q^{-2})^{-1} - 2PA\cos\delta.
\end{aligned}
\tag{22}
$$

Here a and b are assumed to be known. Note that a and b do not depend on angle ϕ, but only on P, A and $\cos\delta$. Using a and b, we can also write simple expressions for p_3^2,

$$p_3^2 = a + \mathrm{i}b, \tag{23}$$

and for p_3,

$$p_3 = \pm\mathcal{P}.\mathcal{V}.\sqrt{a + \mathrm{i}b}. \tag{24}$$

The sign in (24) must, of course, be determined in some other way.

The functions a and b, given by (22), depend on two medium parameters, V and Q, and on four wave propagation quantities, P_1, A_1, P_2, A_2, or on three wave propagation quantities P, A and $\cos\delta$. The isolines of a and b, as functions of P and A, for constant $\cos\delta$, are displayed in Fig. 1. To make certain effects we wish to explain more distinct, a strongly dissipative medium is considered ($V = 1.44$ km/s, Q=2). Quantity $\cos\delta$ is kept constant; it is negative in the upper picture ($\delta = 150^o$) and positive in the lower picture ($\delta = 30^o$). It should again be emphasized that the tangential attenuation angle δ may exceed 90^o, whereas attenuation angle γ is always less than 90^o in a viscoelastic medium.

The isolines of both a and b, for $\cos\delta$ constant, are hyperbolas. Among them a distinct role is played by isolines $a = 0$ and $b = 0$, denoted by bold lines in Fig. 1. As we can see from (22) and from the upper picture in Fig. 1, b is always positive for $\cos\delta \leq 0$. For $\cos\delta > 0$, however, b may be negative, and both isolines $a = 0$ and $b = 0$ exist. See the lower picture in Fig. 1.

A very important role in the whole procedure is played by the point S^*, at which isolines $a = 0$ and $b = 0$ intersect. Consequently, $a = 0$ and $b = 0$ at S^*, square root (24) vanishes, and S^* represents the branch point.

We shall now determine the coordinates of branch point S^* by solving equations $a = 0$ and $b = 0$ for P and A, at fixed $\cos\delta$. We denote these solutions by P^* and A^*. Thus, P^* and A^* satisfy the equations, see (22):

$$V^{-2}(1+Q^{-2})^{-1} = P^{*2} - A^{*2}, \quad V^{-2}Q^{-1}(1+Q^{-2})^{-1} = 2P^*A^*\cos\delta. \tag{25}$$

For fixed $\cos\delta \geq 0$, this yields

$$
\begin{aligned}
P^* &= \frac{1}{\sqrt{2}V(1+Q^{-2})^{1/2}}\left[\sqrt{1+\frac{1}{Q^2\cos^2\delta}}+1\right]^{1/2}, \\
A^* &= \frac{1}{\sqrt{2}V(1+Q^{-2})^{1/2}}\left[\sqrt{1+\frac{1}{Q^2\cos^2\delta}}-1\right]^{1/2}.
\end{aligned}
\tag{26}
$$

But this is exactly the same as (14), only attenuation angle γ has been replaced by the tangential attenuation angle δ. Thus, the tangential phase velocity $\mathcal{C}^*$ is given by the

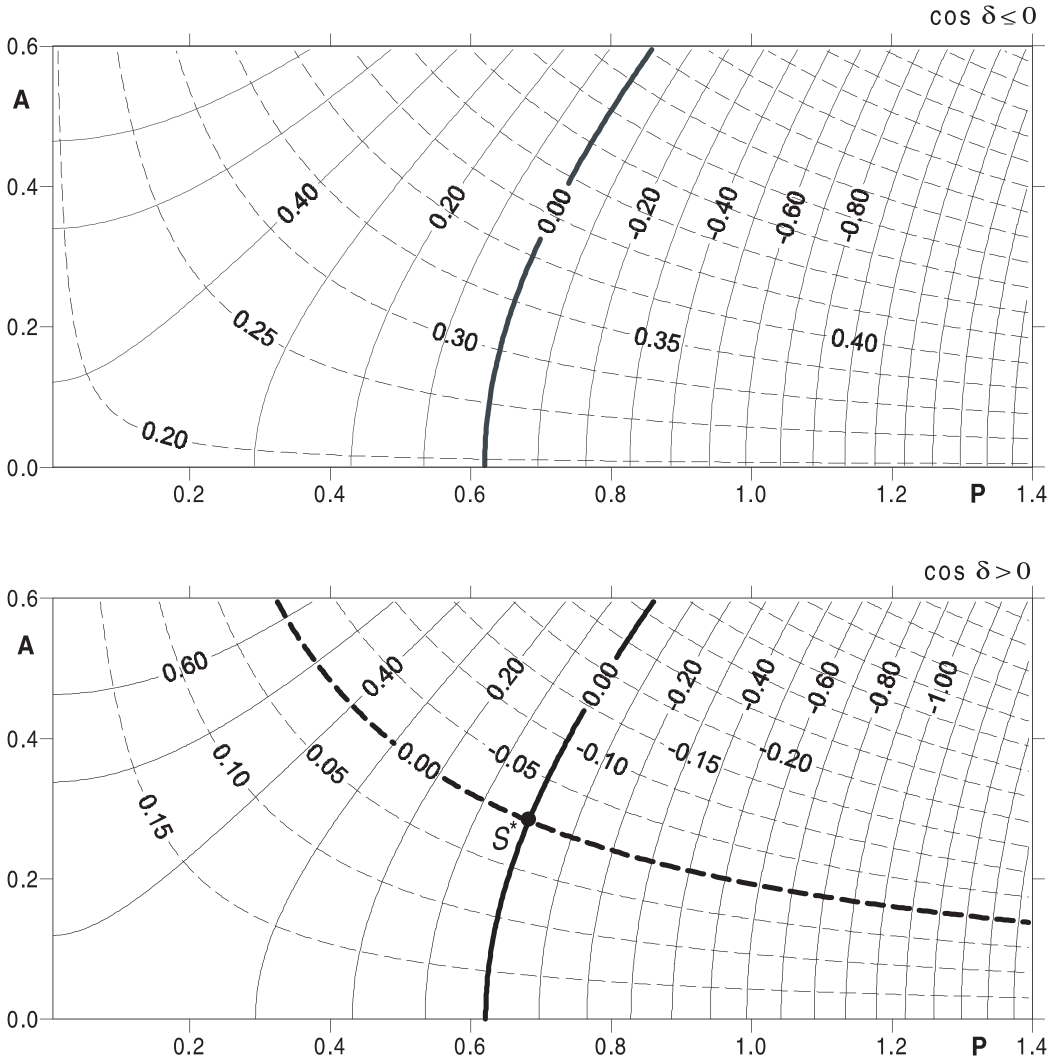

Figure 1: The isolines of a and b, defined by (21), in terms of P and A, for $\cos\delta$ const. Medium parameters: $V = 1.44$ km/s, $Q = 2$. Upper picture: $\cos\delta < 0$ ($\delta = 150^o$). Lower picture: $\cos\delta > 0$ ($\delta = 30^o$). The bold continuous line represents isoline $a = 0$, the bold dashed line isoline $b = 0$, S^* denotes the branch point.

relation

$$\mathcal{C}^* = 1/P^* = \sqrt{2}V(1+Q^{-2})^{1/2}[\sqrt{1+1/Q^2\cos^2\delta}+1]^{-1/2}. \qquad (27)$$

The result is that P^* and A^* are directly related to the tangential (apparent) velocity along Σ.

For $\cos\delta \le 0$, branch point S^* does not exist. The sign "+" in (24) can be used for any P and A in this case. It remains to determine the sign in (24) for $\cos\delta > 0$. Suitable criteria will be proposed in Section 3.

3 Continuity criteria

We shall now express (24) in the following form:

$$p_3 = \epsilon\ \mathcal{P}.\mathcal{V}.\sqrt{a+\mathrm{i}b}. \qquad (28)$$

Here a and b are given by (22), and $\epsilon = \pm 1$. We wish to determine the sign of ϵ.

Before we propose the relevant criteria to determine ϵ, we shall briefly discuss certain properties of $\sqrt{a+\mathrm{i}b}$. We introduce a complex variable $z = a + \mathrm{i}b$, defined on plane $-\infty < a < \infty$, $-\infty < b < \infty$. Thus, z corresponds to p_3^2, see (28). Complex function $\sqrt{z}$ is defined on a two-sheeted Riemannian surface, with a branch point S^* at $z = 0$ (i.e. at $a = 0$, $b = 0$). This branch line runs from $z = 0$ to infinity, and may be chosen in various ways. Here we shall choose the branch line of $\sqrt{z}$ so that it corresponds to the definition of $\mathcal{P}.\mathcal{V}.\sqrt{z}$, i.e. along the negative part of the real axis. Consequently, the branch line is formed by points (a, b), satisfying the relations

$$b = 0, \quad a \le 0. \qquad (29)$$

In the lower picture of Fig. 1, the branch line is situated along the bold dashed line, from S^* to the right. $\mathcal{P}.\mathcal{V}.\sqrt{a+\mathrm{i}b}$ is then uniquely defined on the upper sheet of the Riemannian surface, and $-\mathcal{P}.\mathcal{V}.\sqrt{a+\mathrm{i}b}$ corresponds to the lower sheet of the Riemannian surface.

Let us now consider any continuous parametric line C on the (a, b) plane, $a = a(u)$, $b = b(u)$, parameterized by an arbitrary monotonic parameter u. We shall call it *profile* C. For example, we can define profile C by the parametric equations

$$P_1 = P_1(u), \quad P_2 = P_2(u), \quad A_1 = A_1(u), \quad A_2 = A_2(u), \qquad (30)$$

or by parametric equations

$$P = P(u), \quad A = A(u), \quad \delta = \delta(u). \qquad (31)$$

Here u may be an arbitrary monotonic parameter. For example, u may represent an angle of incidence.

We assume that ϵ is known at the initial point of C, $\epsilon = \epsilon_0$. The initial point of C should be chosen so that $\epsilon = \epsilon_0$ is known. For example, it may correspond to normal incidence (with $\epsilon_0 = 1$). The continuity criterion may then be formulated in the following simple way:

Continuity criterion 1:
Assume that $\epsilon = \epsilon_0$ is known at the initial point of the parametric profile C. Then, moving monotonically along C, the sign of ϵ changes only at those points of profile C at which profile C intersects branch line (29).

Let us add five notes to continuity criterion 1.
a) The criterion may be numerically realized in many ways. The most convenient way is probably based on a point-by-point calculation of ϵ along profile C, taking into account the signs of a and b at these points. Increased care should be devoted to situations in which profile C runs partly or completely along the branch line ($b = 0, a \leq 0$).
b) Profile C is defined in terms of quantities P_1, P_2, A_1 and A_2 (or in terms of P, A and $\cos\delta$), defined along surface Σ. It is not influenced at all by the velocities and the quality factors of the P and S waves in both halfspaces. Consequently, the same procedure may be used to solve the R/T problem at a structural interface, and the initial value problem at an initial surface.
c) If the R/T problem is considered, it would also be possible to use alternative parameters, related directly to the incident wave. Assume that V^{inc}, Q^{inc} are known in the halfspace, in which the incident wave propagates. We can then specify the complex-valued slowness vector of the incident wave by three angles: the angle of incidence i^{inc}, the attenuation angle γ^{inc}, and the tangential attenuation angle δ^{inc}. Analogously, the slowness vector of the selected R/T wave (velocity V, quality factor Q) can then be fully specified by the angle of reflection/transmission i, attenuation angle γ, and the tangential attenuation angle δ.
d) In the actual problems of the structural interface and/or of the initial surface, several square roots are always involved. For example, in the solution of the R/T problem at a structural interface between two viscoelastic halfspaces, four square roots are involved (corresponding to reflected and transmitted, P and S waves). The same profile C must be used to determine all these square roots. The reason is that the determination of all square roots must be considered. Moreover, even the square root corresponding to the incident wave must satisfy the continuity criterion along the common profile.
e) The criterion is quite universal. It may even be used for homogeneous and inhomogeneous plane waves in elastic (non-dissipative) media.

Using continuity criterion 1, we can determine p_3 for all points along profile C. Thus, if we put $p_3 = P_3 + \mathrm{i}A_3$, we obtain

$$P_3 = P_3(P_1, P_2, A_1, A_2), \quad A_3 = A_3(P_1, P_2, A_1, A_2). \tag{32}$$

As we can see from (22), the signs of a and b do not change if all four quantities P_1, P_2, A_1, A_2 change signs. Consequently, P_3 and A_3 determined along profile C are the same for both cases (if also ϵ_0 is the same). We then obtain the following symmetry relations:

$$\begin{aligned} P_3(-P_1, -P_2, -A_1, -A_2) &= P_3(P_1, P_2, A_1, A_2), \\ A_3(-P_1, -P_2, -A_1, -A_2) &= A_3(P_1, P_2, A_1, A_2). \end{aligned} \tag{33}$$

These are very important relations, indicating that p_3 remains the same if the signs of complex-valued p_1 and p_2 are changed. We can speak of "complete backward propagation". It is not sufficient to change the signs of P_1 and P_2, corresponding to the tangential components of the propagation vector, to obtain the symmetrical results. It is also necessary to change the signs of A_1 and A_2, corresponding to the tangential components of the attenuation vector. The consequence of (33) is that the R/T coefficients are the same both for forward and complete backward propagation. The reciprocity of the R/T coefficients also applies to anisotropic media, as was shown by Chapman (1994). Unfortunately, the complete backward propagation is not a standard case in practical applications in viscoelastic media. For example, in the coplanar case, backward propagation at a fixed attenuation angle γ (the same in forward and backward propagation) does not represent the complete backward propagation.

In certain special cases, it is not necessary to use general criterion 1 and to seek the intersection points of profile C with the branch line; it is sufficient to check only the sign of some quantity at any point of the profile. We shall present one such criterion, which is based on quantities P, A and $\cos\delta$, see (18), (19) and (20). We will consider profiles in the (P, A) plane, along which $\phi = const.$ and $\cos\delta = const.$ The most important restriction is that $\cos\delta$ must be constant along the profile. Why do we have to consider $\cos\delta = const.$? As we know from (26), the position of the branch point and of the relevant branch line does not depend on P and A at all, but depends on $\cos^2\delta$. Thus, we have to consider only such profiles along which $\cos^2\delta = const.$ Otherwise, the position of the branch point and of the relevant branch line would be different for different points of the profile. Note that the case of $\cos^2\delta$ along the profile plays an important role in the investigation of wavefields in viscoelastic media. It includes the very important coplanar case of $\cos^2\delta = 1$. Thus, practically all investigations of the R/T process in viscoelastic media, known from the seismological literature, can be included under this case.

We shall now consider an arbitrary, continuous and single-valued curve $A = f(P)$, defined in the quarter-plane $P \in \langle 0, \infty), A \in \langle 0, \infty)$, see Figs. 2 – 5. We shall again call this curve the profile. We assume that $\cos\delta$ is constant along the profile, so that the branch point and relevant branch line are strictly defined and are the same for all points along the profile.

We shall first present three simple examples with simple straight-line profiles $A = const.$, se Figs. 2, 3 and 4. We will use the same medium parameters as in Fig. 1. Thus, Figs. 2, 3 and 4 are directly comparable with Fig. 1, and have the same branch point S^* and branch line as Fig. 1.

Fig. 2 shows profile 1, specified by $A = 0.2$. We consider $\delta = 150^o$ (i.e. $\cos\delta < 0$). The situation is very simple in this case as the branch point does not exist, see the upper picture in Fig. 1, and Fig. 2. Along profile $A = 0.2$, the value of b is positive everywhere. The profile intersects line $a = 0$ at S_a. For the values of a and b along profile 1, see Fig. 2b. Fig. 2c shows the parametric curve $p_3^2 = a + ib$, corresponding to profile $A = 0.2$. The monotonic parameter along the curve is P. The curve is fully situated in the first and second quadrant, and intersects the positive imaginary axis at S_a. The negative real axis (branch line) is not intersected at all. Consequently, p_3 is fully situated in the first quadrant, see Fig. 2d, and $\epsilon = 1$.

For $\cos\delta \geq 0$, the situation is more complicated; both curves $a = 0$ and $b = 0$ are involved. Figures 3 and 4 assume $\delta = 30^o$, so that $\cos\delta > 0$. See also the lower picture of Fig. 1. The branch point S^* in this case is situated at $P^* = 0.68$, $A^* = 0.33$. We shall first consider profile 2, specified by $A = 0.4$, see Fig. 3. At all points along this profile,

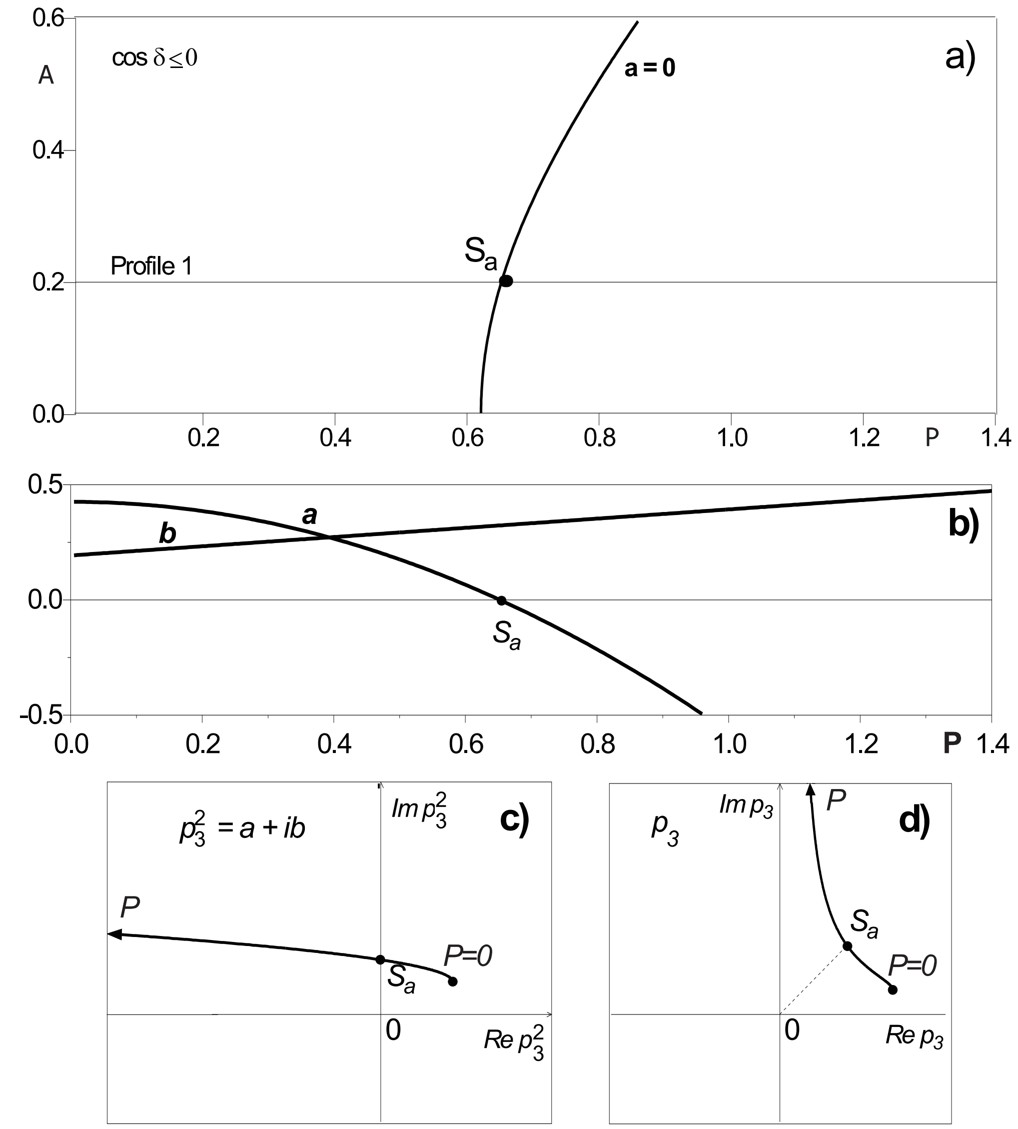

Figure 2: Straight-line profile 1 ($A = 0.2$) in the (P, A) plane, for $\delta = 150^o$ (see also the upper picture of Fig. 1). Fig. 2b shows the values of a and b along profile 1, Fig. 2c the parametric curve $p_3^2 = a + \mathrm{i}b$ in the $(\mathrm{Re}(p_3^2), \mathrm{Im}(p_3^2))$ plane, corresponding to profile 1, and Fig. 2d the parametric curve $p_3 = \sqrt{a + \mathrm{i}b}$ in the $(\mathrm{Re}(p_3), \mathrm{Im}(p_3))$ plane, corresponding to profile 1. The parameter along the curves in Figs. 2c and 2d is P, varying from 0 to infinity.

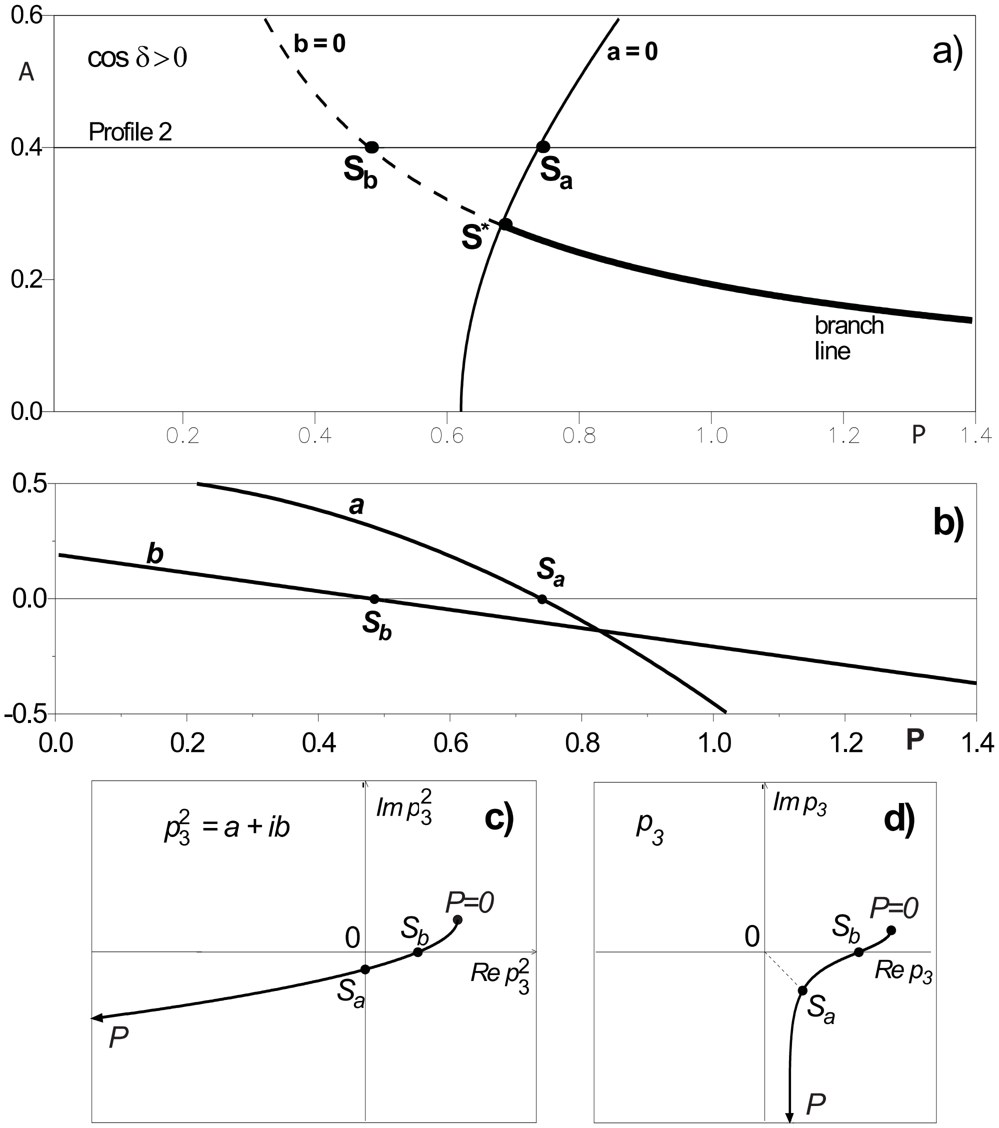

Figure 3: Straight-line profile 2 ($A = 0.4$) in the (P, A) plane, for $\delta = 30^o$ (see also the lower picture of Fig. 1). Point S^* denotes the branch point. Figs. 3b, 3c and 3d have the same meaning as Figs. 2b, 2c and 2d. Note the negative values of $\mathrm{Im}(p_3)$ in Fig. 3d. This implies the exponential increase of amplitudes away from the interface of the generated wave under consideration.

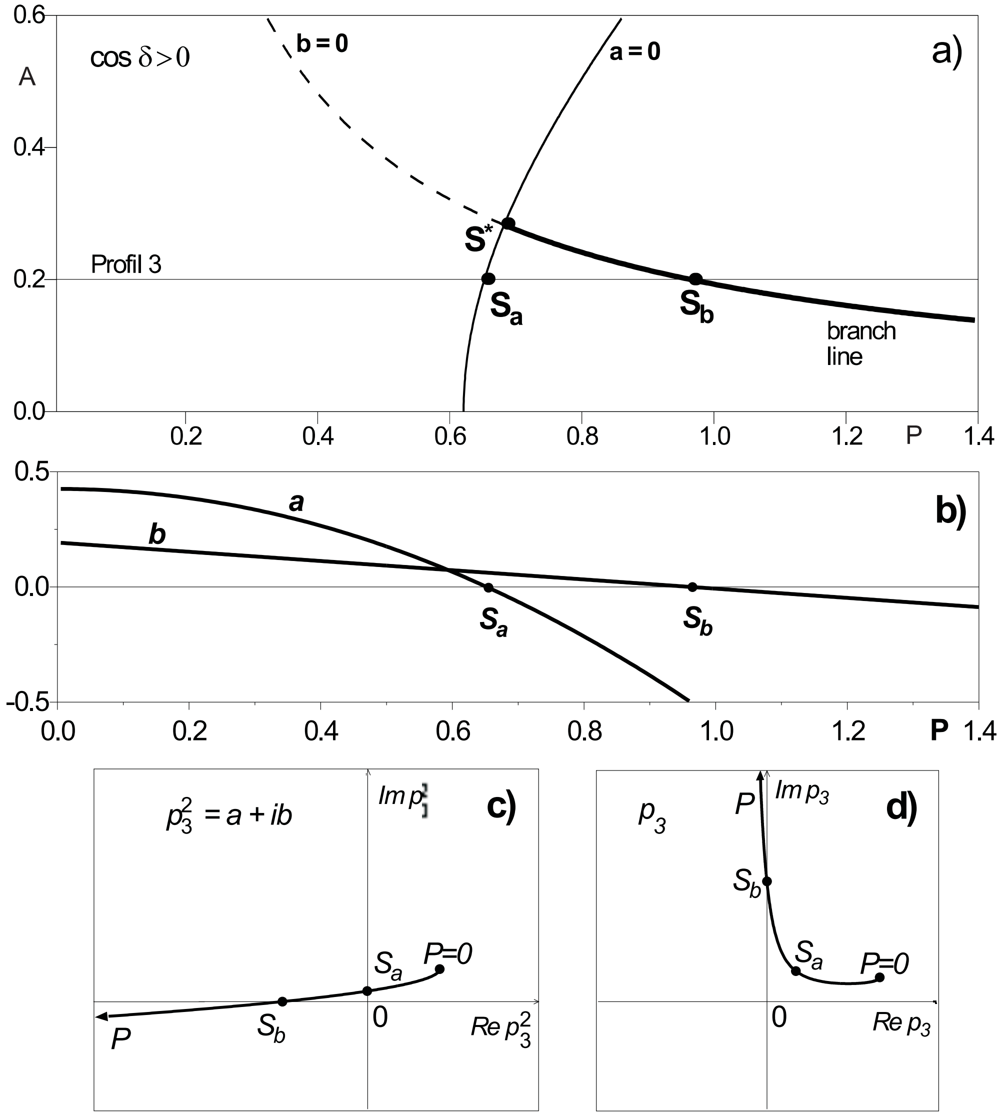

Figure 4: Straight-line profile 3 ($A = 0.2$) in the (P, A) plane, for $\delta = 30^o$ (see also the lower picture of Fig. 1). Point S^* denotes the branch point. Figs. 4b, 4c and 4d have the same meaning as Figs. 2b, 2c and 2d. Note the intersection of the profile with the branch line at S_b, and corresponding negative $\mathrm{Re}(p_3)$ in Fig. 4d. This implies that the R/T propagation angle of the wave under consideration exceeds 90^o for $P > P(S_b)$.

$A > A^*$. The profile first intersects line $b = 0$ at S_b, and after this line $a = 0$ at S_a. Line $b = 0$ at S_b, however, does not represent the branch line in this case. Figure 3c shows the parametric curve $p_3^2 = a + \mathrm{i}b$, corresponding to profile 2, parameterized again by P. For $P = 0$, p_3^2 is situated in the first quadrant, at S_b it moves to the fourth quadrant, and at S_a to the third quadrant. The branch line (negative real axis) is not intersected. Consequently, p_3 is fully situated in the first and fourth quadrants, see Fig. 3d, and $\epsilon = +1$.

There is a basic difference between the results along profiles 1 and 2. Along profile 1, $A_3 = \mathrm{Im}(p_3)$ is always positive, but along profile 2, it is negative for $P > P(S_b)$. The consequence is that the amplitudes decay exponentially away from Σ in the former case, and grow exponentially away from the interface in the latter case.

Finally, we shall treat the "anomalous case", in which the profile intersects the branch line. See profile 3 in Fig. 4, specified by $A = 0.2$. Similarly as in Fig. 3, $\delta = 30^o$, $P^* = 0.68$, $A^* = 0.33$. At all points along the profile, $A < A^*$. In this case the profile first intersects the branch line $a = 0$ at S_a, and then line $b = 0$ at S_b. Line $b = 0$ at S_b now represents a branch line. Fig. 4c shows the parametric curve of $p_3^2 = a + \mathrm{i}b$, corresponding to profile 3 (with parameter P). The curve is more complex than in the previous cases. For $P = 0$, it starts in the first quadrant, at S_a it intersects the positive imaginary axis, and moves to the second quadrant. Finally, at S_b, it intersects the negative real axis (branch line), and moves into the third quadrant. To construct p_3 from p_3^2, it is necessary to take into account that the branch line was crossed at S_b. The parametric curve of p_3 (see Fig. 4d) starts in the first quadrant for $P = 0$, and impinges the positive imaginary axis at S_b. The principal value of $\sqrt{a + \mathrm{i}b}$ would then cause a jump from the positive imaginary axis to the negative imaginary axis. We, however, require a continuous result. For this reason we have to use $\epsilon = -1$ for $P > P(S_b)$.

We shall now consider smooth profiles $A = f(P)$, along which A is not constant. Of course, $\cos\delta$ must be constant along the profile. Whether the profile is situated below the branch point S^* at $P = P^*$ (i.e., $f(P^*) < A^*$), or whether it is situated above the branch point S^* at $P = P^*$, $f(P^*) > A^*$, plays an important role in the criterion, see Fig. 5. First consider the profile situated above the branch point at $P = P^*$, $f(P^*) > A^*$, see the upper picture in Fig. 5. Then $\epsilon = -1$ for $P > P(S_b)$, where the profile intersects the branch line. As $b < 0$ for $P^* < P < P(S_b)$, and $b > 0$ for $P > P(S_b)$, we can conclude that, in this case, we have to use $\epsilon = -1$ if $b > 0$. The situation is different for the profile situated below the branch point at $P = P^*$, $f(P^*) < A^*$, see the lower picture in Fig. 5. Again, $\epsilon = -1$ for $P > P(S_b)$, where the profile intersects the branch line. In this case, however, $b > 0$ for $P^* < P < P(S_b)$ and $b < 0$ for $P > P(S_b)$. Thus, in this case, we have to use $\epsilon = -1$ for $b < 0$.

Now we are prepared to formulate the criterion for the determination of ϵ along profile $A = f(P)$, along which $\cos\delta$ is constant. The criterion applies to the general noncoplanar case.

Continuity criterion 2

Consider a smooth profile $A = f(P)$, along which $\cos\delta = const.$, and assume that the initial point of the profile is situated at $P < P^*$. Then $\epsilon = 1$ at all points of the profile, with the exception of the two following "anomalous" situations:

a) The first anomalous situation is specified by the following four conditions:

$$\cos\delta > 0, \quad P \geq P^*, \quad f(P^*) > A^*, \quad b > 0. \tag{34}$$

b) The second anomalous situation is specified by the following four conditions:

$$\cos\delta > 0, \quad P \geq P^*, \quad f(P^*) < A^*, \quad b < 0. \tag{35}$$

If conditions (a) or (b) are satisfied, then $\epsilon = -1$.

Several notes on continuity criterion 2. The application of the criterion is simple. Assume that V, Q and $\cos\delta$ are given and that the profile is specified by the equation $A = f(P)$. For $\cos\delta \leq 0$, we can use $\epsilon = 1$ along the whole profile. For $\cos\delta > 0$, we first determine the coordinates of branch point S^*, i.e. P^* and A^*, using (26). We further determine $f(P^*)$ and determine whether $f(P^*) > A^*$ or $f(P^*) < A^*$. In other words, we determine whether the profile $A = f(P)$ is situated above or below branch point S^* at $P = P^*$. This can be done once and forever before starting the computations along the profile. After this we merely check whether $b > 0$ or $b < 0$ at any point of the profile, and use (34), (35).

The same criterion, based on (34), (35), applies even if the branch line is intersected by the profile several times. We do not need to bother about multiple intersections of the profile with the branch line at all.

If we wish to consider profiles along which also $\cos\delta$ varies, it is necessary to use general continuity criterion 1 and the profile in the (a, b) plane.

The case of $P_2 = 0$

Without any loss of generality, we can consider $P_2 = 0$ in all previous equations. The case of $P_2 = 0$ may be easily obtained from the general case of $P_2 \neq 0$ by a simple rotation of the Cartesian coordinate system about the x_3-axis. Thus, $P_2 = 0$ may be considered, both for the coplanar and noncoplanar case. Of course, components A_2 do not generally vanish after such a rotation. For $P_2 = 0$, we obtain $\phi = 0$ or $\phi = \pi$ after such a rotation. This yields two possible relations between P_1, A_1, A_2 and P, A, δ, see (18). For $\phi = 0$ we obtain:

$$P_1 = P, \quad A_1 = A\cos\delta, \quad A_2 = A\sin\delta. \tag{36}$$

Similarly, for $\phi = \pi$,

$$P_1 = -P, \quad A_1 = -A\cos\delta, \quad A_2 = -A\sin\delta. \tag{37}$$

For both these cases, we obtain for a and b:

$$\begin{aligned} a &= V^{-2}(1+Q^{-2})^{-1} - P_1^2 + A_1^2 + A_2^2 = V^{-2}(1+Q^{-2})^{-1} - P^2 + A^2, \\ b &= V^{-2}Q^{-1}(1+Q^{-2})^{-1} - 2P_1A_1 = V^{-2}Q^{-1}(1+Q^{-2})^{-1} - 2PA\cos\delta. \end{aligned} \tag{38}$$

The expression for $\cos\delta$ now simplifies to

$$\cos\delta = P_1A_1/PA. \tag{39}$$

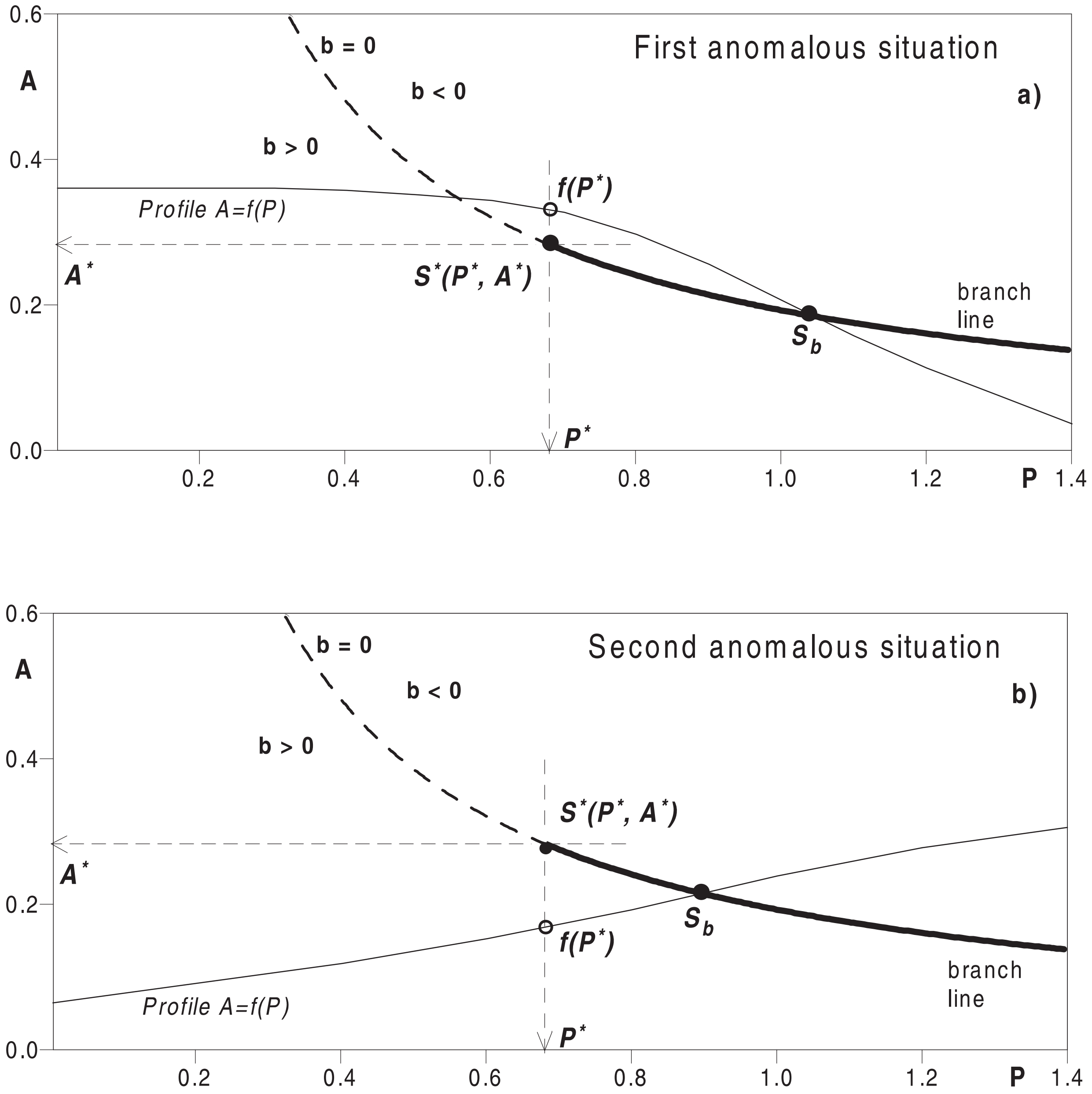

Figure 5: Curved profiles $A = f(P)$ in the (P, A) plane. Point S^* represents the branch point. In the upper picture, the profile runs above the branch point, and intersects the branch line at S_b from above (from $b < 0$ to $b > 0$). In the lower picture, the profile runs below the branch point, and intersects the branch line at S_b from below (from $b > 0$ to $b < 0$).

Moreover,

$$P = |P_1|, \quad A = \sqrt{A_1^2 + A_2^2}. \tag{40}$$

The coordinates of the branch point, P^* and A^*, are again given by (26). They depend only on $\cos\delta$, not on P and A. Thus, $\cos\delta$ should be fixed along the whole profile.

Of course, continuity criteria 1 and 2 also apply for $P_2 = 0$. In continuity criterion 2, we can use the condition $P_1 A_1 > 0$ instead of $\cos\delta > 0$ in (34) and (35).

4 Examples and discussion

We shall now present several examples of computations of P_3 and A_3 from values P_1, A_1, P_2 and A_2, known along plane Σ. Without any loss of generality, we shall consider the case of $P_2 = 0$. The model under consideration is the same as in Figs. 1 – 4, i.e. $V = 1.44$ km/s and $Q = 2$. We shall present actual computations of P_3 and A_3 along profiles 2 and 3, shown in Figs. 3 and 4. In all cases, A_1 and A_2 are assumed to be constant, and P_1 to vary from -1.4 to 1.4. Quantity P_1 may be related to the angle of incidence i^{inc}, if we wish. The case of $P_1 > 0$ then corresponds to the positive angles of incidence i^{inc}, and $P_1 < 0$ to the negative angles of incidence. The actual relation between P_1 and the angle of incidence i^{inc} depends on V^{inc}, Q^{inc} and γ^{inc}, where γ^{inc} is the attenuation angle of the incident wave. The range of P_1 used in Figs. 6 – 8, $-1.4 < P_1 < 1.4$, is mostly broader than the range of the real-valued angles of incidence i^{inc}, $-90^o < i^{inc} < 90^o$.

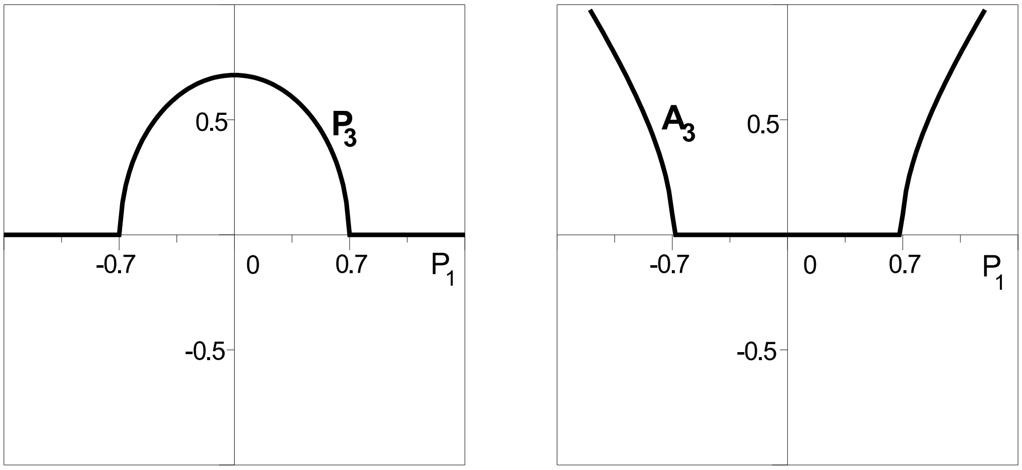

Figure 6: Curves $P_3 = P_3(P_1)$ and $A_3 = A_3(P_1)$ in perfectly elastic models ($Q^{-1} = 0$), for the homogeneous incident wave ($A_1 = A_2 = 0$). The curves have a well-known shape. In the subcritical region ($|P_1| < 0.69$), $P_3 \geq 0$ and $A_3 = 0$. Consequently, the R/T propagation angle is always less than 90^o. In the postcritical region ($|P_1| > 0.69$), $P_3 = 0$ and $A_3 \geq 0$. Consequently, the amplitudes of the inhomogeneous R/T waves always decay exponentially away from the interface.

Before we present and discuss the results for viscoelastic models, we shall present, for reference, the analogous curves for homogeneous incident plane waves ($A_1 = A_2 = 0$) in perfectly elastic models ($Q^{-1} = 0$). See Fig. 6. The curves in Fig. 6 have a well-known shape. The critical value of P_1 is $1/V = 0.6944; |P_1| < 0.6944$ corresponds to the subcritical region, and $|P_1| > 0.6944$ to the postcritical region. In the subcritical region ($|P_1| < 0.6944$), the normal component of p_3 of the slowness vector is real-valued ($A_3 = 0$). Analogously, in the postcritical region ($|P_1| > 0.6944$), the normal component p_3 is purely imaginary ($P_3 = 0$). Both P_3 and A_3 are nonnegative. Moreover, they are both symmetrical with respect to P_1, around point $P_1 = 0$. Consequently, in the elastic case and for $A_1 = A_2 = 0$, the amplitudes of the generated wave under consideration always decay exponentially away from the interface in the postcritical region.

Now we shall discuss curves $P_3 = P_3(P_1)$ and $A_3 = A_3(P_1)$ for viscoelastic models ($V = 1.44$ km/s, $Q = 2$), see the bold lines in Figs. 7 and 8. Fig. 7 corresponds to the computations along profile $A = 0.4$ of Fig. 3, and Fig. 8 to the computations along profile $A = 0.2$ of Fig. 4. The values of A_1 and A_2 are always taken constant along the whole profile. They are $A_1 = \pm 0.2$ and $A_2 = 0.3464$ in Fig. 7, and $A_1 = \pm 0.1, A_2 = 0.1732$ in Fig. 8. The upper pictures in Figs. 7 and 8 correspond to positive A_1, and the lower pictures to negative A_1.

In all the pictures of Figs. 7 and 8, continuity criterion 2 (with $P_2 = 0$) was used to determine the sign of ϵ. It should be noted that, if A_1 is fixed, $\cos\delta$ has different signs for $P_1 > 0$ and $P_1 < 0$, see (39). Actually, $\cos\delta = \pm 0.5236$, that is, $\delta = 30^o$ or $\delta = 150^o$. Thus, the region of P_1 under consideration, $-1.4 < P_1 < 1.4$, is divided into two regions, $0 \leq P_1 < 1.4$ and $-1.4 < P_1 \leq 0$, and criterion 2 is applied to these two regions independently. In one of these regions we always have $\cos\delta < 0$, so that $\epsilon = 1$ automatically. In the second region we have to check the sign of ϵ using criterion 2.

Two additional thin curves are also displayed in all pictures of Figs. 7 and 8. These curves do not correspond to the medium considered in Figs. 1 – 4. The continuous thin line corresponds to the inhomogeneous waves in the relevant perfectly elastic medium (with $Q^{-1} = 0$), and the dashed thin line to the inhomogeneous waves in the viscoelastic medium with a higher, more realistic Q ($Q = 10$). It is not surprising to see that the curves for $Q^{-1} = 0.1$ are considerably closer to the elastic case ($Q^{-1} = 0$) than the bold curves for $Q^{-1} = 0.5$.

It is not difficult to verify that continuity criterion 2 yields $\epsilon = 1$ in all the situations in Fig. 7. Consequently, P_3 is always positive in Fig.7. In Fig. 8, however, the continuity criterion dictates the change of sign of ϵ for $P_1 \doteq 0.96$ if $A_1 > 0$, and for $P_1 \doteq -0.96$ if $A_1 < 0$. See also Fig. 4, which clearly displays the intersection of the profile with the branch line at $P = 0.96$. In Figs. 7 and 8, negative P_3 are obtained only in strongly dissipative media ($Q^{-1} = 0.5$, bold lines). For nondissipative media ($Q^{-1} = 0$), the situation with negative P_3 was not observed.

The case of $P_3 < 0$ looks paradoxical. In this case, the propagation vector $\mathbf{P}$ of the generated wave under consideration is pointing back into the interface. There is, however, nothing paradoxical in this fact, if inhomogeneous plane waves in viscoelastic media are considered. The propagation of inhomogeneous waves in a viscoelastic medium is a considerably more complicated process than the propagation of homogeneous waves in perfectly elastic models, and it cannot be interpreted solely in terms of the real-valued

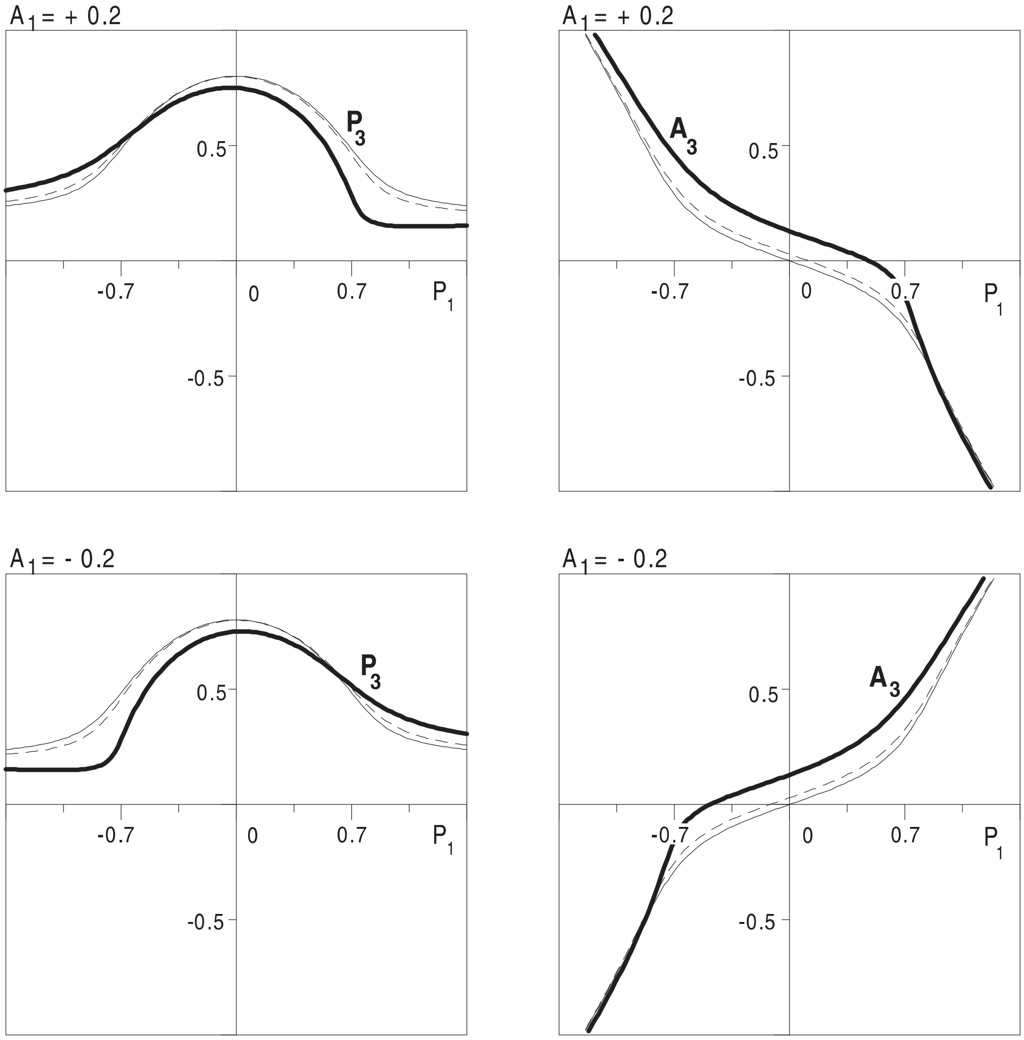

Figure 7: Curves $P_3 = P_3(P_1)$ and $A_3 = A_3(P_1)$, computed along the straight-line profile $A = 0.4$ shown in Fig. 3. The bold lines correspond to inhomogeneous plane waves in viscoelastic media ($V = 1.44$ km/s, $Q = 2$), the thin dashed lines to inhomogeneous plane waves in viscoelastic media with higher Q's ($V = 1.44$ km/s, $Q = 10$), and the thin continuous lines to inhomogeneous plane waves in perfectly elastic media ($V = 1.44$ km/s, $Q^{-1} = 0$). Note the asymmetricity of the bold curves for positive and negative P_1. For a more detailed discussion, see text.

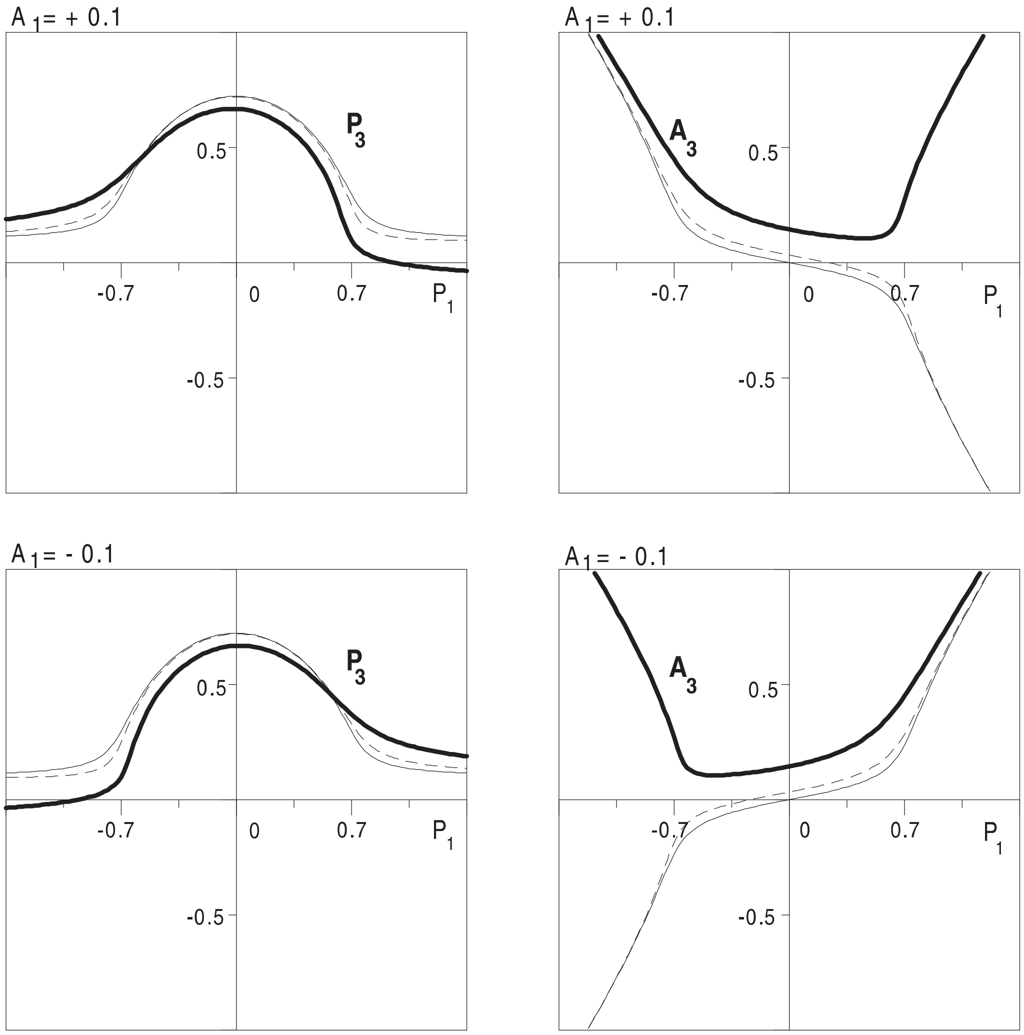

Figure 8: Curves $P_3 = P_3(P_1)$ and $A_3 = A_3(P_1)$, computed along the straight-line profile $A = 0.2$ shown in Fig. 4. The meaning of the individual curves is the same as in Fig. 7. Note the negative values of P_3 for $P_1 > 0.96$ (if $A_1 > 0$), and for $P_1 < -0.96$ (if $A_1 < 0$). These negative values of P_3 correspond to the R/T propagation angles exceeding 90^o.

propagation vector $\mathbf{P}$. A similar situation with $P_3 < 0$ is also well known in perfectly elastic anisotropic media, where the real-valued propagation vector of the generated wave may point back into the interface.

The next point of interest is the direction of the exponential decay of amplitudes of waves generated at a structurel interface in viscoelastic media (away or towards the interface). This direction is fully controlled by the sign of A_3. For $A_3 > 0$, the amplitudes decay exponentially away from the interface, and for $A_3 < 0$ they grow exponentially away from the interface. Both these possibilities are fully admissible for inhomogeneous plane waves, both in viscoelastic and elastic media. As we can see in Figs. 7 and 8, the behaviour of curves $A_3 = A_3(P_1)$ is very diverse in viscoelastic media. A_3 is positive for certain P_1, and negative for some other P_1. Curve $A_3 = A_3(P_1)$ may also be completely positive, for all P_1, see Fig. 8. The situation may be even more complex if A_1 and A_2 varying along the profile were considered.

For inhomogeneous plane waves propagating in perfectly elastic media ($Q^{-1} = 0$), and for A_1 and A_2 fixed, curves $P_3 = P_3(P_1)$ and $A_3 = A_3(P_1)$ are symmetric or antisymmetric; see the continuous thin lines in Figs. 7 and 8. For weakly dissipative media (Q^{-1} very small, but nonvanishing), curves $P_3 = P_3(P_1)$ and $A_3 = A_3(P_1)$ are very close to those of $Q^{-1} = 0$, i.e. close to the symmetric or antisymmetric. See the thin dashed lines in Figs. 7 and 8. For strongly dissipative media, however, the deviations of $P_3(P_1)$ from symmetry and of $A_3(P_1)$ from antisymmetry may be considerably more pronounced.

In the previous examples of this section, shown in Figs. 7 and 8, we have only considered profiles, along which A was constant. As explained in Section 3, it is simple to apply continuity rule 2 even to any profile specified by a continuous single-valued function $A = f(P)$, along which $\cos\delta$ is constant. Note that profile $A = const.$ intersects the branch line maximum once, but profile $A = f(P)$ may intersect the branch line several times. Consequently, P_3 may be negative in some finite regions of P_1, and positive in some other regions. To demonstrate the applicability of our criteria to such a case, we shall consider the well-known example given by Krebes (1984), see also Brokešová and Červený (1998, 2001) and Brokešová (2001). Krebes discussed a coplanar case, in which $P_2 = 0$ and $A_2 = 0$, and in which P_1 and A_1 are expressed in terms of the parameters of the incident wave as follows:

$$P_1 = |P_1| \sin i^{inc}, \quad A_1 = |A_1| \sin(i^{inc} - \gamma^{inc}). \tag{41}$$

Here i^{inc} is the angle of incidence and γ^{inc} the attenuation angle of the incident wave. Moreover, $|P_1|$ and $|A_1|$ are given by (14), where all parameters correspond to the incident wave. Krebes (1984) proposed a criterion to determine ϵ along a profile $0 \leq i^{inc} \leq 90^o$, for γ^{inc} const. He showed that ϵ was negative for $i^{inc} > i_1$, where i_1 is the so-called critical angle of incidence. He further showed that, in some cases, also a second critical angle i_2 exists, at which again the sign of ϵ changes to positive. (The analytical expressions for i_1 and i_2 can be found in Brokešová and Červený, 1998.) This situation is clearly demonstrated in Fig. 9. Profile $A = f(P)$ was computed using (41), considering $P = |P_1|, A = |A_1|$, and $\cos\delta = 1$. Medium parameters close to those chosen by Krebes (1984) were used ($V^{inc} = 1.44$ km/s, $Q^{inc} = 13, \gamma^{inc} = -50^o, V = 2.08$ km/s, $Q = 5$). Note that Q, corresponding to the transmitted wave, is lower than Q^{inc}, corresponding to the incident wave ($Q = 5, Q^{inc} = 13$). The coordinates of branch point S^* are given by (26), and are as follows: $P^* = 0.4808, A^* = 0.0476$. Fig. 9 clearly demonstrates two intersections of the profile with the branch line. Inbetween both intersections, ϵ is negative, and otherwise it is positive. Consequently, the propagation vector of the transmitted wave is oriented towards the interface only for angles of incidence between these intersections. Both for smaller and larger angles of incidence, it is oriented away from the interface.

5 Concluding remarks

The procedures proposed in this paper can also be used in solving the point source - plane interface problem in viscoelastic media. At a specified receiver point, the exact integral solution can be expressed in the form of a double integral over p_1 and p_2. This integral can be calculated numerically (reflectivity method), or approximately, using asymptotic high-frequency methods. To simplify the explanation, we shall consider only a single integral, with $p_2 = 0$. The application of asymptotic methods consists in the deformation of the original integration contour in the complex plane $p_1 = P_1 + \mathrm{i}A_1$ into other suitable contour(s) passing through the saddle point(s) of the complex-valued travel-time function (steepest descent contours). Any saddle point is, in general, complex-valued. It depends not only on the medium parameters, but also on the position of the source and receiver. The position of the saddle points yields the complex-valued stationary value of p_1 (the "ray parameter"), $p_1^s = P_1^s + \mathrm{i}A_1^s$. Consequently, the component A_1 of the attenuation vector at the source cannot be taken freely as an additional parameter of the problem; it is influenced by the position of the source and the receiver. Moreover, "ray parameter" p_1 is complex-valued, so that the rays of R/T waves, connecting the source and the receiver, are complex-valued curves (the coordinates of points along the rays are complex numbers). For more details, see Hearn and Krebes (1990a, b). Hearn and Krebes refer to these complex rays as *stationary rays*, and show that the real-valued travel time corresponding to the stationary ray is the smallest among the travel times corresponding to all possible complex-valued rays connecting the source and receiver. Thus, the stationary ray also satisfies Fermat's principle of least time. For more details on complex rays in viscoelastic media, see Thomson (1997) and Kravtsov, Forbes and Asatryan (1999), where many other references can be found.

In the deformation of the original integration contour into the new contour of steepest descent, the endpoints of both contours should be the same, and must be situated on the same sheet of the Riemannian surface. If the new contour of the steepest descent crosses the branch line, it is necessary to add contributions corresponding to the branch line integrals. It is well known that the branch line integrals yield contributions corresponding to head waves. Consequently, the properties of the head waves propagating along the interface between two viscoelastic media are controlled by the position of the branch points and relevant branch lines in the complex plane $p_1 = P_1 + \mathrm{i}A_1$.

Analogous complex rays are also obtained if the problem of the initial surface-point receiver is being solved in viscoelastic media.

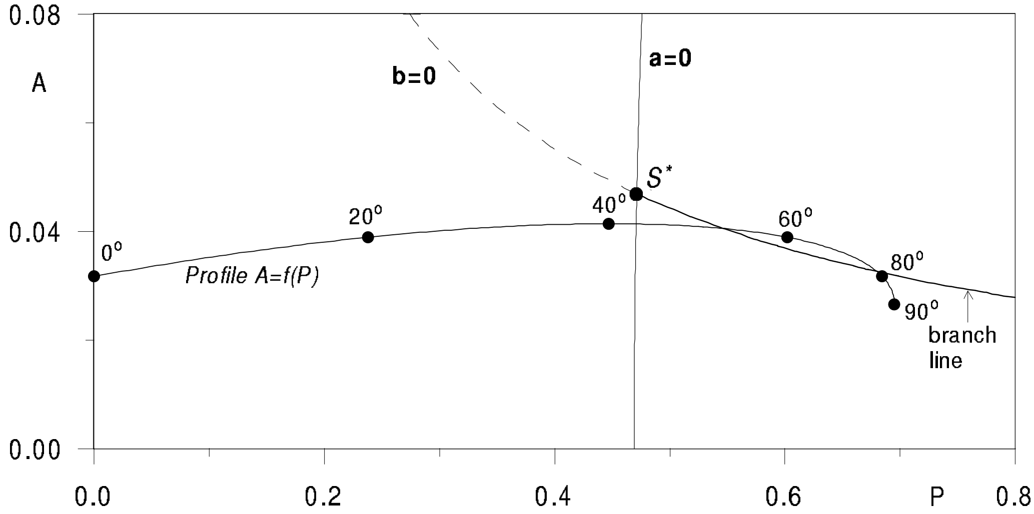

Figure 9: Example of two intersections of the profile $A = f(P)$ with the branch line. Inbetween both intersections, P_3 is negative, otherwise it is positive. In other words, the R/T propagation angle exceeds 90^o inbetween both intersections, otherwise it is less than 90^o.

Acknowledgements

This research has been supported by the Consortium Project "Seismic Waves in Complex 3-D Structures" and by the MŠMT research project J13/98-113200004.

References

Ainslie, M.A., and Burns, P.W. (1995). Energy conserving reflection and transmission coefficients for a solid-solid boundary, *J. Acoust. Soc. Am.*, **98**, 2836 – 2840.

Auld, B.A. (1990). Acoustic fields and waves in solids, New York: Wiley.

Borcherdt, R.D. (1973). Energy and plane waves in linear viscoelastic media, *J. Geophys. Res.*, **78**, 2242 – 2533.

Borcherdt, R.D. (1977). Reflection and refraction of Type-II S waves in elastic and anelastic media, *Bull. seismol. Soc. Am.* , **67**, 43 – 67.

Borcherdt, R.D. (1982). Reflection-refraction of general P- and Type-I S-waves in elastic and anelastic solids, *Geophys. J. R. astr. Soc.* , **70**, 621 – 638.

Brokešová, J. (2001). Reflection/transmission coefficients at a plane interface in dissipative and non-dissipative isotropic media: A comparison, *J. Comput. Acoustics*, **9**, 623 – 641.

Brokešová, J., and Červený, V. (1998). Inhomogeneous plane waves in dissipative, isotropic and anisotropic media. Reflection/transmission coefficients, in *Seismic waves in complex 3-D structures*, Report 7, pp. 57 – 146. Prague: Faculty of Mathematics and Physics, Charles University. (Available online at "http://sw3d.mff.cuni.cz/".)

Brokešová, J., and Červený, V. (2001). Energy conservation equations and interaction contributions at a structural interface between two dissipative media. Numerical experiments, in *Seismic waves in complex 3-D structures*, Report 11, pp. 315 – 336. Prague: Faculty of Mathematics and Physics, Charles University. (Available online at "http://sw3d.mff.cuni.cz/".)

Brokešová, J., and Červený, V. (2002). Viscoelastic R/T problem for arbitrary orientation of propagation and attenuation vectors. *Extended Abstracts of Papers, EAEG 64th Conference and Exhibition*, Florence, in press.

Buchen, P.W. (1971). Reflection, transmission and refraction of SH waves in linear viscoelastic solids, *Geophys. J. R. astr. Soc.* , **25**, 97 – 113.

Carcione, J.M. (2001). *Wave fields in real media: Wave propagation in anisotropic, anelastic and porous media*, Amsterdam: Pergamon Press.

Caviglia, G., and Morro, A. (1992). *Inhomogeneous waves in solids and fluids*, Singapore: World Scientific.

Červený, V. (2001). *Seismic ray theory*, Cambridge: Cambridge Univ. Press.

Chapman, C.H. (1994). Reflection/transmission coefficients reciprocities in anisotropic edia, *Geophys. J. Int.*, **116**, 498 – 501.

Deschamps, M. (1990). Réflexion-réfraction de l'onde plane hétérogène: Répartition de l'énergie, *J. Acoustique*, **3**, 251 – 261.

Deschamps, M. (1994). Reflection and refraction of the evanescent plane wave on plane interfaces, *J. Acoust. Soc. Am.*, **96**, 2841 – 2848.

Hearn, D.J., and Krebes, E.S. (1990a). On computing ray-synthetic seismograms for anelastic media using complex rays, *Geophysics* , **55**, 422 – 432.

Hearn, D.J., and Krebes, E.S. (1990b). Complex rays applied to wave propagation in a viscoelastic medium, *Pure and Appl. Geophys.*, **132**, 401 – 415.

Koesoemadinata, A.P., and McMechan, G.A. (2001a). Empirical estimation of viscoelastic seismic parameters from petrophysical properties of sandstone, *Geophysics* , **66**, 1457 – 1470.

Koesoemadinata, A.P., and McMechan, G.A. (2001b). Sensitivity of viscoelastic reflection amplitude variation with angle to petrophysical properties, *J. Seis. Exploration*, **9**, 269 – 284.

Kravtsov, Yu.A., Forbes, G.W., and Asatryan, A.A. (1999). Theory and applications of complex rays, in *Progress in optics*, vol. 39, pp. 1 – 61, ed. E. Wolf. Amsterdam: North Holland.

Krebes, E.S. (1983). The viscoelastic reflection-transmission problem: Two special cases, *Bull. seismol. Soc. Am.* , **73**, 1673 – 1684.

Krebes, E.S. (1984). On the reflection and transmission of viscoelastic waves — Some numerical results, *Geophysics* , **49**, 1374 – 1380.

Richards, P.G. (1981). On wavefronts and interfaces in anelastic media, *Bull. seismol. Soc. Am.* , **74**, 2157 – 2165.

Thomson, C.J. (1997). Complex rays and wave packets for decaying signals in inhomogeneous, anisotropic and anelastic media, *Studia geoph. et geod.*, **41**, 345 – 381.